Journal of Inflammation Research

Dovepress
Taylor & Francis Group

Open Access Full Text Article

ORIGINAL RESEARCH

Decrease of NAD^+ Inhibits the Apoptosis of OLP T Cells via Inducing Mitochondrial Fission

Zhuo-Yu Zhang[1], Fang Wang[1,2], Gang Zhou[1,3]

[1]State Key Laboratory of Oral & Maxillofacial Reconstruction and Regeneration, Key Laboratory of Oral Biomedicine Ministry of Education, Hubei Key Laboratory of Stomatology, School & Hospital of Stomatology, Wuhan University, Wuhan, People's Republic of China; [2]Center for Cariology, Endodontics and Periodontics, Optical Valley Branch, School & Hospital of Stomatology, Wuhan University, Wuhan, People's Republic of China; [3]Department of Oral Medicine, School and Hospital of Stomatology, Wuhan University, Wuhan, People's Republic of China

Correspondence: Fang Wang, Center for Cariology, Endodontics and Periodontics, Optical Valley Branch, School & Hospital of Stomatology, Wuhan University, Wuhan, People's Republic of China, Email wangfang-nm@whu.edu.cn; Gang Zhou, Department of Oral Medicine, School and Hospital of Stomatology, Wuhan University, Wuhan, People's Republic of China, Email zhougang@whu.edu.cn

Purpose: Oral lichen planus (OLP) is a chronic, immune-mediated inflammatory disease involving T cells. Mitochondrial fission plays a crucial role in T cell fate through structural remodeling. Nicotinamide adenine dinucleotide (NAD^+) regulates mitochondrial remodeling and function. This study explored the role of NAD^+ in modulating mitochondrial fission and apoptosis in T cells under the OLP immune-inflammatory environment.

Patients and Methods: T cells and plasma were isolated from peripheral blood. Mitochondrial morphology was characterized by transmission electron microscopy and Mito-Tracker staining. OLP plasma-exposed Jurkat T cells were infected with the Drp1 shRNA virus to investigate the role of mitochondrial fission in OLP T cell apoptosis. OLP T cells and OLP plasma-exposed Jurkat T cells were treated with either β-nicotinamide mononucleotide (an NAD^+ synthesis precursor) or FK866 (an NAD^+ synthesis inhibitor) to assess the effect of NAD^+ regulation on mitochondrial remodeling and T cell apoptosis.

Results: OLP T cells exhibited fragmented mitochondria with elevated dynamin-related protein 1 (Drp1) and reduced mitofusin 2 (Mfn2) expression, accompanied by decreased apoptosis. Drp1 knockdown in OLP plasma-exposed Jurkat T cells increased apoptosis and reduced proliferation. NAD^+ levels were reduced in both OLP T cells and OLP plasma-treated Jurkat T cells, leading to enhanced mitochondrial fission, decreased mitochondrial membrane potential (MMP) and respiration function, and reduced apoptosis rate. β-nicotinamide mononucleotide supplementation restored NAD^+ levels, suppressed mitochondrial fission, improved MMP, and promoted apoptosis in these cells.

Conclusion: Reduced NAD^+ levels in OLP T cells enhanced mitochondrial fission and contributed to decreased apoptosis. NAD^+ supplementation mitigated these effects, suggesting a potential therapeutic strategy for restoring T cell homeostasis in OLP.

Keywords: mitochondria, nicotinamide adenine dinucleotide, T cells, oral lichen planus

Introduction

Oral lichen planus (OLP) is a chronic, immune-inflammatory disease affecting the oral mucosa,[1] with a prevalence ranging from 0.1% to 4% in the general population and a higher incidence among middle-aged women.[1,2] The World Health Organization (WHO) classifies OLP as an oral potentially malignant disease.[3] The histological features of OLP include a dense subepithelial infiltration of lymphocytes and liquefactive degeneration in the basal keratinocytes.[4,5] Although OLP's pathogenesis remains unclear, evidence suggests it involves T cell-mediated immune dysregulation.[2,4] T cells dynamically regulate their energy metabolism to fulfill immune functions in diverse diseases.[6,7] Our previous study demonstrated elevated lactate dehydrogenase levels in the glycolytic pathway in OLP T cells.[8] While mitochondria-dominated energy metabolism supports T cell survival, T cells predominantly use glycolysis under high-glucose conditions, promoting cell proliferation and Th17 cell differentiation.[9] Thus, mitochondria play a crucial role in energy metabolism, which depends on the structural integrity of mitochondria.[10] However, the structural and functional characteristics of mitochondria in OLP T cells are not yet fully understood.

Received: 22 October 2024
Accepted: 12 January 2025
Published: 23 January 2025

As dynamic organelles, mitochondria perform metabolic functions and adapt to extracellular environments through mitochondrial structural remodeling.[10,11] They continuously alter their shape through fission, fusion, and other dynamic processes, including branching, debranching, stretching, and contraction.[12] Among these processes, mitochondrial fission is well-characterized.[12] Mitochondrial fission generally reduces oxidative phosphorylation sites, forcing cellular energy metabolism to shift to glycolysis.[13] Mitochondrial morphology is diverse and can appear as small spheres, ellipsoids, short or elongated tubes, and reticular networks depending on the regulation of fission or other structural remodeling processes.[14] Dynamin-related protein 1 (Drp1) is a key regulator of mitochondrial fission; however, mitochondrial fusion is controlled by dynamin-related GTPases, including mitofusin 1 (MFN1) and mitofusin 2 (MFN2) on the outer mitochondrial membrane (OMM) and optic atrophy protein 1 (OPA1) on the inner mitochondrial membrane (IMM).[11] Structural remodeling of mitochondria plays a pivotal role in various autoimmune diseases. For instance, mitochondrial fission genes are upregulated in Sjogren's syndrome.[15] In addition, Drp1 depletion in T cells inhibited mitochondrial fission, improving symptoms in both systemic lupus erythematosus (SLE) patients and lupus-susceptible mice.[16] In a mouse model of autoimmune encephalitis, accumulation of mitochondrial fission in regulatory T (Treg) cells resulted in severely aberrant mitochondrial morphology with mitochondrial dysfunction.[17] Abnormal mitochondrial membrane potential (MMP) is a hallmark of mitochondrial respiration dysfunction.[16] In patients with primary progressive multiple sclerosis, T cell mitochondria appeared smaller and more spherical, with reduced mass and MMP, decreasing mitochondrial respiration.[18]

Nicotinamide adenine dinucleotide (NAD^+) is a crucial cofactor in various redox reactions, including glycolysis, the tricarboxylic acid (TCA) cycle, oxidative phosphorylation (OXPHOS), fatty acid oxidation (FAO), and serine biosynthesis.[19] NAD^+ metabolism is a highly dynamic process, and all four NAD coenzymes (NAD^+, NADH, $NADP^+$, and NADPH) serve redox and signaling functions.[20] In addition to redox cycling, NAD^+ is synthesized and consumed through distinct pathways, with dietary precursors such as nicotinamide (Nam), nicotinamide riboside (NR), nicotinamide mononucleotide (NMN), and niacin (vitamin B3) contributing to its biosynthesis.[20] NMN inhibits Drp1-mediated mitochondrial fragmentation through Sirtuin 3 (SIRT3)-dependent mechanisms.[21] Recent studies have highlighted the role of NAD^+ in regulating mitochondrial function and its potential significance in the pathogenesis of immune diseases. For example, NAD^+ precursors improved mitochondrial biogenesis and reduced aberrant mitochondrial fission in a mouse model of mitochondrial myopathy, delaying disease progression.[22] Additionally, according to previous studies, NAD^+ can restore mitochondrial function, attenuate the activation of the inflammatory pathway, including interferon and nuclear factor-κB signaling, and reduce immune cell infiltration.[23] The increased NAD^+ levels can potentially enhance mitochondrial respiration and reduce NOD-like receptor thermal protein domain-associated protein 3 (NLRP3) inflammasome and pro-inflammatory cytokine production in peripheral blood mononuclear cells (PBMCs).[24] NAD^+ supplementation also improved T cell mitochondrial homeostasis and alleviated inflammation in mice.[25] These findings underscore the link between NAD^+ levels, mitochondrial dynamics, and inflammatory states.

This study investigated the role of NAD^+ in regulating mitochondrial fission and apoptosis in T cells in the OLP immune-inflammatory environment. The findings revealed that OLP T cells exhibited increased mitochondrial fission alongside reduced NAD^+ levels. OLP plasma, which provided an inflammatory stimulus, induced mitochondrial fission in Jurkat T cells by depleting NAD^+. In Drp1 knockdown Jurkat T cells cultured in OLP plasma, apoptosis increased while proliferation decreased. Notably, NAD^+ supplementation effectively reversed mitochondrial fission, restored mitochondrial respiratory function, and induced apoptosis in both OLP and Jurkat T cells cultured with OLP plasma.

Materials and Methods

Patients and Samples

Peripheral blood and plasma samples of OLP patients and normal controls were obtained from the Department of Oral Medicine, School and Hospital of Stomatology, Wuhan University. OLP patients were enrolled based on predefined inclusion and exclusion criteria.[9] Table 1 presents the clinical characteristics. This study's protocol adhered to the ethical guidelines outlined in the Declaration of Helsinki and was approved by the Ethics Committee of the Wuhan University School of Stomatology and Hospital (Approval Number: 2022A30).

Table 1 Clinical Characteristics of Subjects

	OLP	Normal Control
Total number	28	21
Gender		
Male	9	6
Female	19	15
Age (years)		
Range	21–68	24–62
Mean ± SD	47 ± 12	49 ± 10

Abbreviations: OLP, Oral Lichen Planus; SD, Standard Deviation.

Isolation of T Cells and Plasma from Peripheral Blood

A heparin blood collection vessel was used to obtain a venous blood sample from each subject. First, peripheral blood was centrifuged at 1550 ×g for 15 min to separate plasma. Then, PBMCs were isolated through density gradient centrifugation using a Ficoll-Hypaque solution (Catalog # LTS1077, Haoyang, China). Subsequently, T cells were isolated from PBMCs using a Human Pan T cell isolation kit (Catalog # Flosep-C-003N, STEMERY, China) according to the instructions provided. Extraction purity of primary T cells was detected by FITC-anti-CD3 monoclonal antibody (mAb) (Catalog # 555339, BD Biosciences, USA) under flow cytometry with CyExpert v2.4 software (Beckman Coulter, USA) (Figure S1A).

Cell Culture

Primary T cells and Jurkat T cells (Cowin Biotech, China) were cultured in RPMI 1640 medium (Catalog # C11875500BT, Thermofishe, China) supplemented with 10% fetal bovine serum (FBS) (Catalog # 11011, Tianhang, China) at a concentration of 5×10^5 cells/mL at 37°C and 5% CO_2. Primary T cells were activated by 1 μg/mL anti-CD3 mAb (Catalog # 317326, Biolegend, USA), 2 μg/mL anti-CD28 mAb (Catalog # 302934, Biolegend, USA), and 50 U/mL Interleukin (IL)-2 (Catalog #I7908, Sigma, Germany) for 72 h. The in vitro proliferation and growth of primary T cells were observed by microscopy (Figure S1B). Jurkat T cells were activated by 1 μg/mL anti-CD3 mAb and 2 μg/mL anti-CD28 mAb for 72 h.

The NAD^+ salvage pathway heavily depends on nicotinamide phosphoribosyl transferase (NAMPT) and nicotinamide mononucleotide adenylyl transferase (NMNAT) enzymes. β-nicotinamide mononucleotide (NMN) serves as a precursor in NAD^+ synthesis, which is subsequently converted into NAD^+ by NMNAT.[26] FK866, a highly selective noncompetitive NAMPT inhibitor, effectively blocks NAD^+ synthesis.[27] Activated primary T cells were cultured in 6-well plates (Catalog # TC 703002, NEST, China) and stimulated with 0.5 mM NMN (Catalog # HY-F0004, MedChem Express NJ, USA) or 50 nM FK866 (Catalog # HY-F50876, MedChem Express NJ, USA) for 48 h. Concerning activated Jurkat T cells, plasma was used to replicate the immune-inflammatory environment of OLP, enabling these cells to more accurately exhibit OLP-like T cell behavior. Thus, activated Jurkat T cells were cultured in 6-well plates at a concentration of 1×10^6 cells/mL, using either OLP or normal plasma, and were simultaneously stimulated with 0.5 mM NMN or 50 nM FK866 for 48 h.

Vector Construction

The Drp1 knockdown lentiviral vector (Lv-shDrp1) and the corresponding lentiviral negative control (NC) were constructed by Shanghai Genechem Co., Ltd. The Drp1 gene is homologous to the human DNM1L (Dynamin-1-like gene), GENE_ID 10059, GenBank accession number NM_012063. Three constructs of Lv-shDrp1 were designed to target different sequences of the Drp1 gene. The target sequences were as follows: Lv-shDrp1#1 (120,103–1),

CGAGATTGTGAGGTTATTGAA; Lv-shDrp1#2 (120,104–12), CGGTGGTGCTAGAATTTGTTA; Lv-shDrp1#3 (120,-105–2), GCTACTTTACTCCAACTTATT. The constructed vectors were confirmed by qPCR and sequencing. The expression and knockdown efficiency of Drp1 were validated in Jurkat T cells using RT-qPCR and Western blotting (WB), followed by selecting a stable knockdown cell line for further functional experiments.

Transmission Electron Microscope Analysis

T cells from OLP patients and normal controls were fixed overnight in a solution containing 2.5% glutaraldehyde, 0.1% potassium ferricyanide, and 1% osmium tetroxide at 4°C. Following dehydration with a graded ethanol series, the samples were embedded in Spurr's epoxy resin and sectioned into ultrathin slices. The sections were stained with 2% uranyl acetate and examined using transmission electron microscopy (TEM, HT-7700, Hitachi, Japan).

Mito-Tracker Red CMXRos Staining and Mito-Tracker Green Staining

T cells (1×10^6) were centrifuged at 1000 ×g for 5 min and incubated in a solution of Mito-Tracker Red CMXRos (100nM, Catalog # C1049B Beyotime, China) or Mito-Tracker Green (100 nM) (Catalog # C1048, Beyotime, China) for 30 min according to the manufacturer's instructions and detected under a laser confocal microscope (Leica, TCS SP8, Germany). T cells stained with Mito-Tracker Green were detected using flow cytometry, and data were analyzed with mean fluorescence intensity (MFI) using CytExpert 2.4 (Beckman, USA).

Mitochondrial Membrane Potential Assay

Following the manufacturer's instructions, T cells were prepared at a concentration of 1×106 cells/mL for MMP assay using an Enhanced Mitochondrial Membrane Potential Assay Kit with JC-1 (Catalog # C2003S, Beyotime, China). Staining was visualized through fluorescence microscopy (Olympus Corporation, Japan).

NAD^+ Assay

T cells were prepared at a concentration of 1×10^6 cells/mL to detect the intracellular level of NAD^+ using Amplite® Fluorimetric NAD Assay Kit (Catalog # 15280, AAT Bioquest, USA) according to the manufacturer's instructions. Increased fluorescence was monitored with a fluorescence plate reader at 420/480 nm.

Western Blot Analysis

T cells were lysed using RIPA buffer (Catalog # G2002, Servicebio, Wuhan, China). Lysates were sonicated and centrifuged at 12000 ×g for 20 min at 4°C. Protein concentrations were quantified using bicinchoninic acid (Catalog # AL006, ACE, China) according to the manufacturer's instructions. Protein samples were separated on a 10% SDS-PAGE gel (Bio-Rad, Poland) and transferred to polyvinylidene difluoride membranes (Millipore, USA). Non-specific binding sites were blocked by incubating with 5% nonfat milk in Tris-buffered saline Tween-20 (TBST) buffer for 1.5 h at room temperature. The membranes were then incubated overnight at 4°C with primary antibodies, followed by washing with TBST and subsequent incubation with goat anti-mouse or goat anti-rabbit secondary IgG antibodies (1:8000, Catalog # M21001, M21002, Abmart, China) for 1 h. Table 2 lists the information on antibodies used in this study. Immunoreactive bands were visualized using an enhanced chemiluminescence kit (Catalog # PMK003, Pumoke, China) and detected by chemiluminescence Odyssey Fc Imaging System (LICOR Biosciences, NE, USA). The bands were quantified by densitometry using ImageJ.

Real-Time Quantitative PCR (qRT-PCR)

RNA was isolated from Jurkat T cells using E.Z.N.A.® Total RNA Kit I (Catalog # R6834-0, Omega Bio-tek, Inc., USA), according to the manufacturer's instructions. HisyGo RT Red SuperMix for qPCR (+gDNA Wiper) (Catalog # RT101, Vazyme, China) was applied to produce the complementary DNA (cDNA) using 1000 ng of total RNA. The mRNA expression was quantified by qRT-PCR using the ChamQ Blue Universal SYBR qPCR Master Mix (Catalog # q312, Vazyme, China). Table 3 lists primer sequences for Drp1 and β-actin (Sangon Biotech Co., Ltd.,

Table 2 The Information of Antibodies Used in This Study

Antibody	Application	Source	Dilution
Mfn2	WB	Abcam (AB124773)	1:1000
Drp1	WB	Abcam (AB124773)	1:1000
β-Actin	WB	Biopm (PMK058)	1:5000
mtTFA	WB	Diagbio (db11961)	1:2000
Caspase-9	WB	Diagbio (db14222)	1:1000
Caspase-3	WB	Abmart (T40044)	1:1000

Abbreviations: Mfn2, Mitofusin 2; Drp1, Dynamin-related protein 1; β-Actin, Beta-Actin; mtTFA, Mitochondrial Transcription Factor A; WB, Western Blot analysis.

Table 3 The Information of Primer Sequences in This Study

Gene	Primer Sequences
Drp1	F: 5′-CTGCCTCAAATCGTCGTAGTG-3′ R: 5′-GAGGTCTCCGGGTGACAATTC-3′
β-Actin	F: 5′-AAGATGACCCAGATCATGTTTGAGACC-3′ R: 5′-AGCCAGGTCCAGACGCAGGAT-3′

Abbreviations: Drp1, Dynamin-related protein 1; β-Actin, Beta-Actin.

Shanghai, China). qRT-PCR data were analyzed using the comparative cycle threshold (CT) method and calculating 2−ΔΔCT.

Apoptosis Assay

T cells were prepared at a concentration of 1×10^6 cells/mL for the apoptosis assay using Annexin V-FITC/PI Apoptosis Kit (Catalog # E-CK-A211, Elabscience, China), according to the manufacturer's instructions. Flow cytometry analysis was performed on apoptotic cells using a Beckman flow cytometer (Beckman, USA).

EdU Cell Proliferation Staining

EdU cell proliferation staining was applied using an EdU kit (BeyoClick™ EdU Cell Proliferation Kit with Alexa Fluor 488, Catalog # CS0071, Beyotime, China). T cells were prepared at a concentration of 1×10^6 cells/mL for the EdU cell proliferation staining, according to the manufacturer's instructions. The cells were subsequently incubated with Hoechst 33342 for 10 min. Fluorescence microscopy (Olympus Corporation, Japan) was used to visualize staining.

Statistical Analysis

GraphPad Prism 8 (GraphPad Software) was used for statistical analysis, and corresponding graphs were generated. Data were presented as mean ± SD. One-way ANOVA was used for pairwise comparisons of the multiple groups, and a two-tailed *t*-test was used to determine statistical significance. Non-parametric Mann–Whitney U and Kruskal–Wallis tests were applied if datasets failed the D'Agostino & Pearson normality test or Shapiro–Wilk normality test. Experiments were repeated at least 3 times. Statistical significance was defined at $P < 0.05$.

Results

OLP T Cells Showed Increased Mitochondrial Fission

T cells of OLP mainly exhibited small and fragmented mitochondria in the cytoplasm. In contrast, T cells of normal controls mainly had large and tubular mitochondria under TEM (Figure 1a). Mito-Tracker Red CMXRos can selectively label bioactive mitochondria, displaying mitochondrial morphology by confocal laser scanning microscopy (CLSM).[28] In OLP T cells, mitochondria labeled with Mito-Tracker Red appeared granular; however, those in normal controls exhibited a more diffuse or cloud-like appearance (Figure 1b). The granular appearance indicated potential mitochondrial fragmentation into smaller units, whereas the cloudier appearance in controls suggested intact, networked mitochondria. The mitochondrial mass in OLP T cells, assessed by the mean fluorescence intensity (MFI) of Mito-Tracker Green,[7] was significantly lower ($P = 0.0196$, Figure 1c and d). Additionally, the mitochondrial fission protein Drp1 was elevated ($P = 0.0119$); however, the fusion protein Mfn2 was reduced ($P = 0.0418$) in OLP T cells compared to controls (Figure 1e and f). These findings collectively indicated increased mitochondrial fission in OLP T cells.

NAD^+ Inhibited Mitochondrial Fission and Promoted Apoptosis of OLP T Cells

To explore the factors contributing to mitochondrial fission in OLP T cells, NAD^+ levels were assessed, which were significantly reduced in these cells ($P = 0.0315$, Figure 2a). NMN, a precursor for NAD^+ synthesis, shifted the mitochondria in OLP T cells from a granular to a cloud-like appearance, indicating a reversal of mitochondrial fragmentation. In contrast, treatment with FK866, an NAD^+ synthesis inhibitor, did not change the granular appearance in OLP T cells. Similarly, in normal control T cells, the mitochondria remained cloudy following NMN treatment; however, they shifted to a granular appearance after FK866 treatment (Figure 2b). Furthermore, the apoptosis rate, as indicated by Annexin V+/PI- staining, in OLP T cells was significantly lower than that of normal controls ($P = 0.0317$). Treatment with NMN significantly increased apoptosis in OLP T cells ($P = 0.0217$, Figure 2c and d). These findings suggest that the elevated mitochondrial fission observed in OLP T cells may be linked to reduced intracellular NAD^+ levels, possibly contributing to decreased apoptosis in these cells.

OLP Plasma Stimulation Induced Mitochondrial Fission of Jurkat T Cells by Decreasing Intracellular NAD^+

Jurkat T cells, an immortalized human T lymphocyte cell line, can be readily cultured and manipulated.[29] These cells were stimulated with OLP and normal plasma to investigate the induction of intracellular NAD^+ levels. NAD^+ levels decreased significantly in Jurkat T cells cultured in OLP plasma compared to those cultured in normal plasma ($P = 0.0185$, Figure 3a). Treatment with NMN effectively elevated NAD^+ levels in Jurkat T cells exposed to both OLP and normal plasma. In contrast, FK866 reduced NAD^+ levels under both conditions ($P < 0.05$, Figure 3a). These findings indicate that OLP plasma induced a decrease in NAD^+ levels in Jurkat T cells, similar to the effect seen in OLP T cells.

Furthermore, mitochondria in Jurkat T cells cultured with OLP plasma primarily exhibited a small and fragmented morphology, similar to that of OLP T cells. In contrast, Jurkat T cells cultured in normal plasma displayed large tubular mitochondria (Figure 3b). After adding NMN to the OLP plasma, the mitochondria in Jurkat T cells adopted tubular structures. In comparison, treatment with FK866 in normal plasma resulted in small and fragmented mitochondria (Figure 3b). Mito-Tracker Red CMXRos staining confirmed granular mitochondria in Jurkat T cells cultured with OLP plasma and cloudy mitochondria in those cultured with normal plasma. Treatment with NMN converted the mitochondria in OLP plasma-cultured Jurkat T cells to a long tubular form. In contrast, treatment with FK866 made the mitochondria in normal plasma-cultured cells appear granular (Figure 3c). The MFI of Mito-Tracker in OLP plasma-cultured Jurkat T cells was significantly lower than that in cells cultured with normal plasma ($P = 0.0012$), and NMN treatment restored the MFI in OLP plasma-cultured cells ($P = 0.0068$, Figure 3d).

Moreover, OLP plasma-cultured Jurkat T cells exhibited higher Drp1 expression ($P = 0.0252$) than those cultured in normal plasma. Treatment with NMN decreased Drp1 expression in OLP plasma-cultured Jurkat T cells ($P < 0.05$, Figure 3e and f). Collectively, these findings indicate that OLP plasma induced mitochondrial fission in Jurkat T cells by reducing NAD^+ levels and that mitochondrial structure remodeling was regulated by NAD^+ levels.

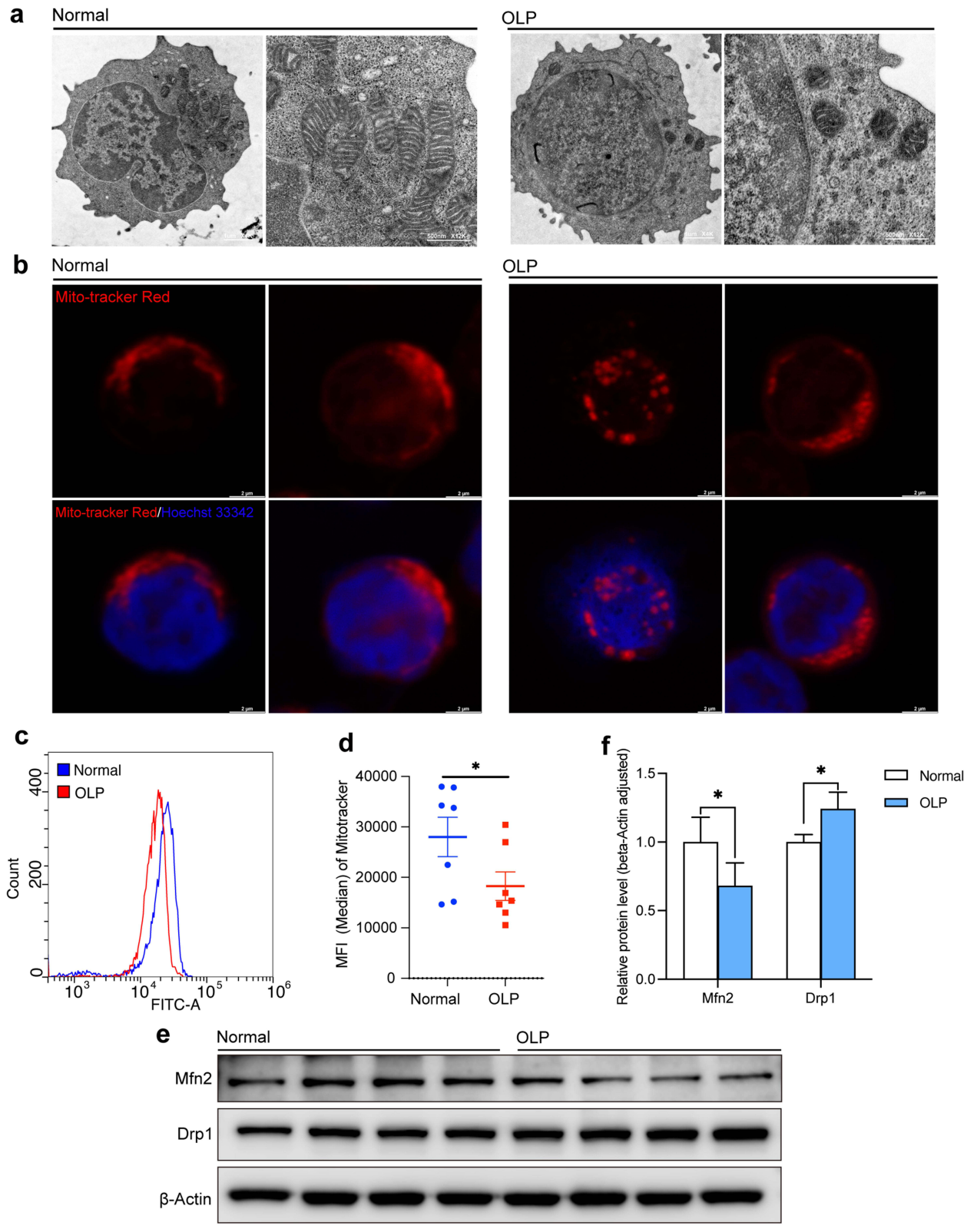

Figure 1 Mitochondrial fission in OLP T cells. (**a**) Representative transmission electron microscopy (TEM) images of mitochondrial morphology in peripheral blood T cells from OLP patients (n = 10) and normal controls (n = 5). Scale bars: 2 μm for ×4.0k magnification and 500 nm for ×12.0k magnification. (**b**) Representative images of Mito-Tracker Red CMXRos staining in peripheral blood T cells from OLP patients (n = 6) and normal controls (n = 6), observed by laser confocal microscopy. Scale bar: 1 μm. (**c**) Representative images of Mito-Tracker Green MFI in OLP and normal T cells, detected by flow cytometry. (**d**) MFI (median) analysis of Mito-Tracker Green in OLP (n = 7) and normal control (n = 7) T cells. (**e**) Representative Western blot images of Mfn2 and Drp1 expression. (**f**) Grey-scale analysis of Mfn2/β-actin and Drp1/β-actin ratios (n = 3). *$P < 0.05$ vs Normal.
Abbreviations: OLP, Oral Lichen Planus; MFI, Mean Fluorescence Intensity.

https://doi.org/10.2147/JIR.S502273

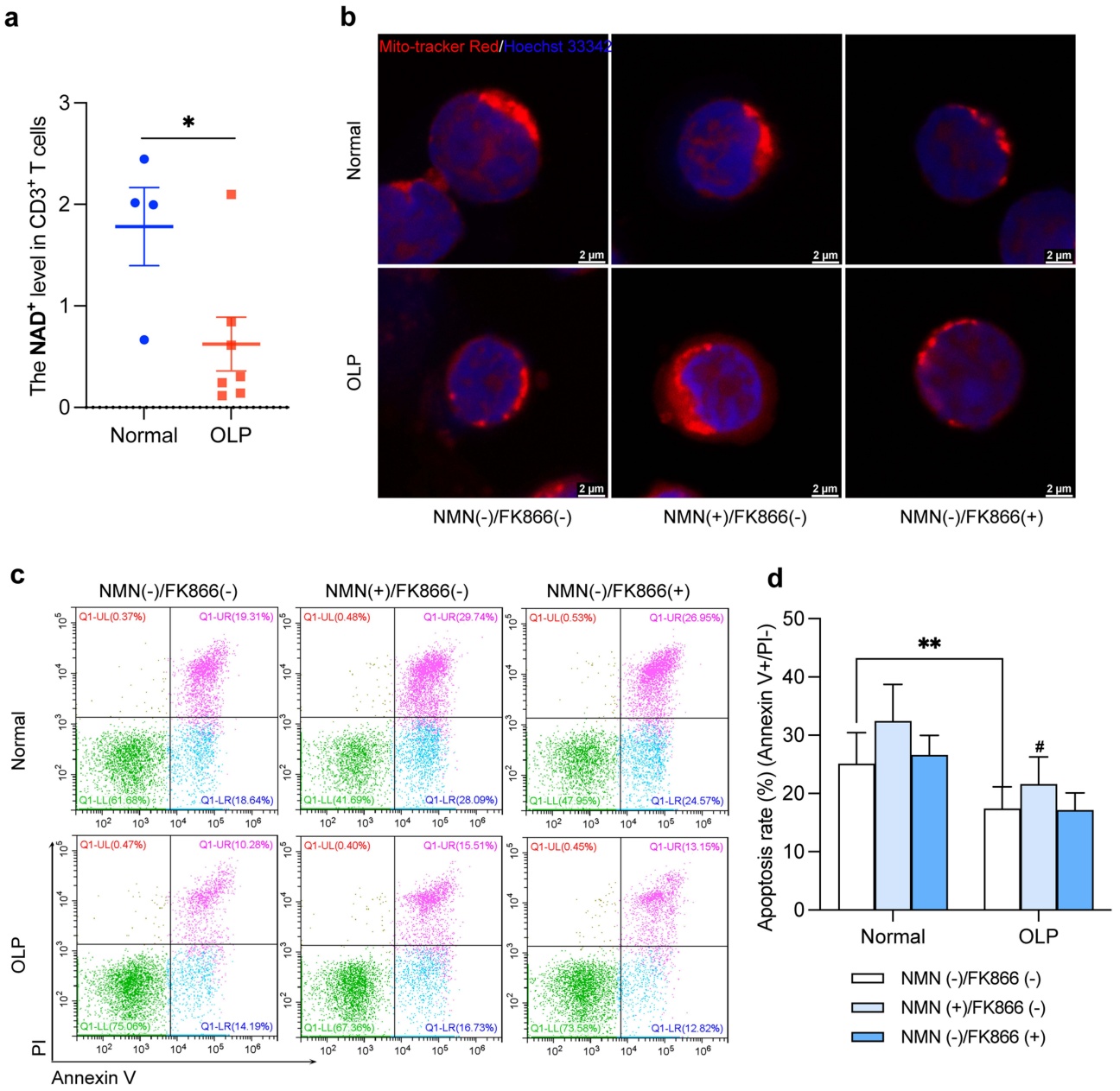

Figure 2 Effect of NAD^+ on mitochondrial fission and apoptosis in OLP T cells. (**a**) NAD^+ levels in OLP (n = 6) and normal (n = 4) T cells. T cells were stimulated with NMN (0.5 mM) or FK866 (50 nM) for 48 h. (**b**) Representative Mito-Tracker Red CMXRos staining images of peripheral blood T cells from OLP patients (n = 6) and normal controls (n = 6), observed by laser confocal microscopy. Scale bar: 2 μm. (**c**) Apoptosis rates of OLP and normal T cells (n = 6), detected by flow cytometry. (**d**) Histogram of apoptosis rates (Annexin V+/PI-) in OLP and normal T cells. $^*P < 0.05$, $^{**}P < 0.01$ vs Normal, $^{\#}P < 0.05$ vs OLP with NMN (-)/FK866 (-).

Abbreviations: OLP, Oral Lichen Planus; NAD^+, Nicotinamide Adenine Dinucleotide; NMN, β-nicotinamide mononucleotide; PI, Propidium Iodide; MFI, Mean Fluorescence Intensity.

Mitochondrial Fission Mediated by Drp1 Inhibited Apoptosis and Promoted Proliferation in Jurkat T Cells Cultured with OLP Plasma

Jurkat T cells were infected with either a negative control virus or shRNA targeting the Drp1 gene to investigate the effect of mitochondrial fission on apoptosis and proliferation of OLP T cells. All three shRNAs significantly reduced Drp1 expression ($P < 0.05$, Figure 4a-c). The sh-Drp1#3 Jurkat T cell line was selected for subsequent experiments to investigate apoptosis. The apoptosis rate in the sh-NC group stimulated with OLP plasma was significantly lower than in the sh-NC group with normal plasma ($P = 0.0312$, Figure 4d and e). Conversely, the apoptosis rate in the sh-Drp1 group

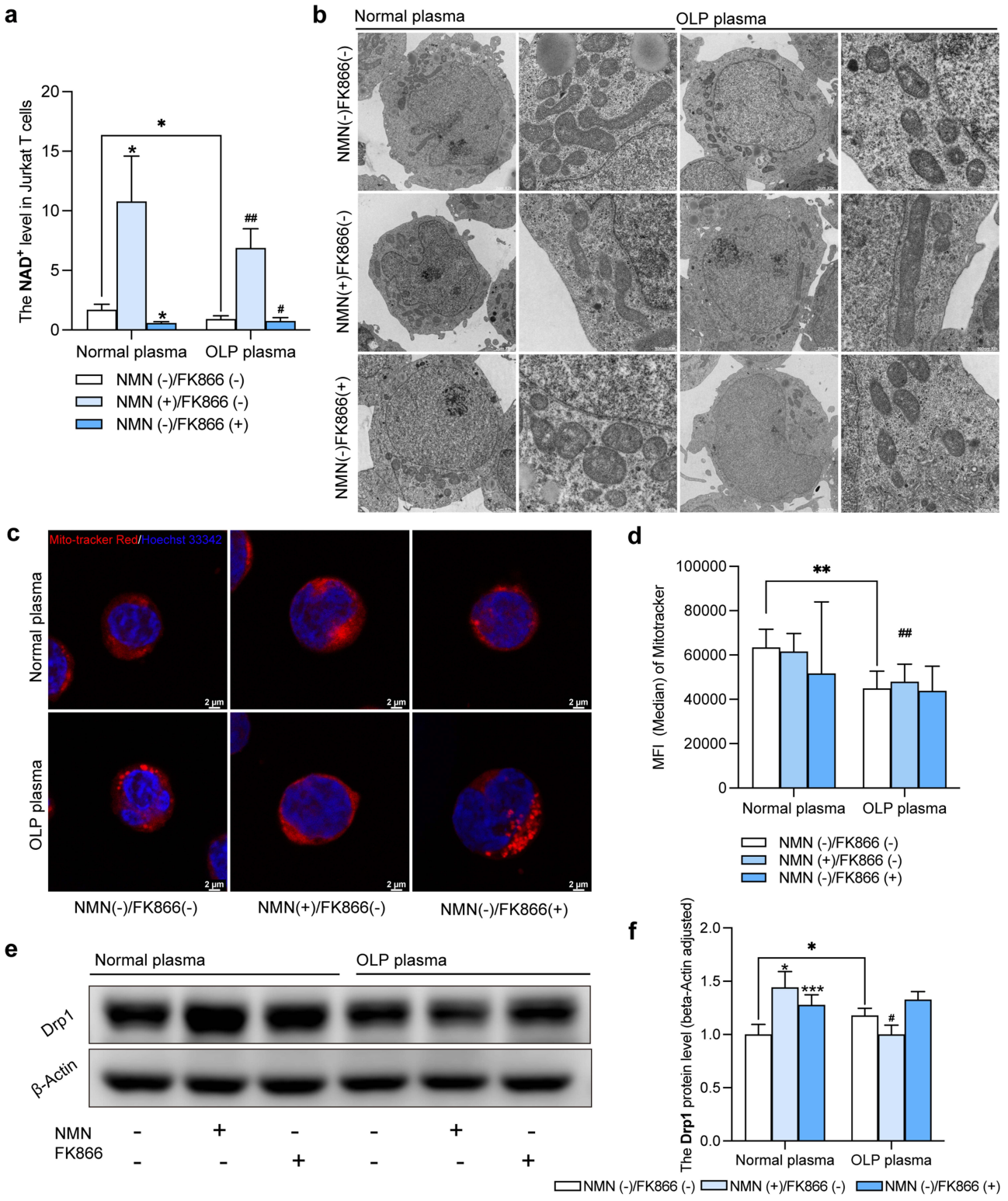

Figure 3 Effect of OLP plasma stimulation and NAD^+ levels on mitochondrial fission. Activated Jurkat T cells were cultured in OLP or normal plasma and stimulated with NMN (0.5 mM) or FK866 (50 nM) for 48 h. (**a**) NAD^+ levels in Jurkat T cells cultured in OLP and normal plasma (n = 3). (**b**) Representative TEM images of mitochondrial morphology in Jurkat T cells cultured in OLP or normal plasma (n = 3). Scale bars: 2 μm for ×2.0k magnification and 1 μm for ×8.0k magnification. (**c**) Representative Mito-Tracker Red CMXRos staining images in Jurkat T cells cultured in OLP or normal plasma (n = 6), observed by laser confocal microscopy. Scale bar: 5 μm. (**d**) MFI (median) of Mito-Tracker Green in Jurkat T cells cultured in OLP or normal plasma (n = 6), detected by flow cytometry. (**e**) Representative Western blot images of Drp1 expression. (**f**) Grey-scale analysis of Drp1/β-actin ratios (n = 3). $^*P < 0.05$, $^{**}P < 0.01$, $^{***}P < 0.001$ vs Normal plasma, $^{\#}P < 0.05$, $^{\#\#}P < 0.01$ vs OLP plasma with NMN (-)/FK866 (-).
Abbreviations: OLP, Oral Lichen Planus; NAD^+, Nicotinamide Adenine Dinucleotide; β-Actin, Beta-Actin; Drp1, Dynamin-related protein 1; NMN, β-nicotinamide mononucleotide; MFI, Mean Fluorescence Intensity.

https://doi.org/10.2147/JIR.S502273

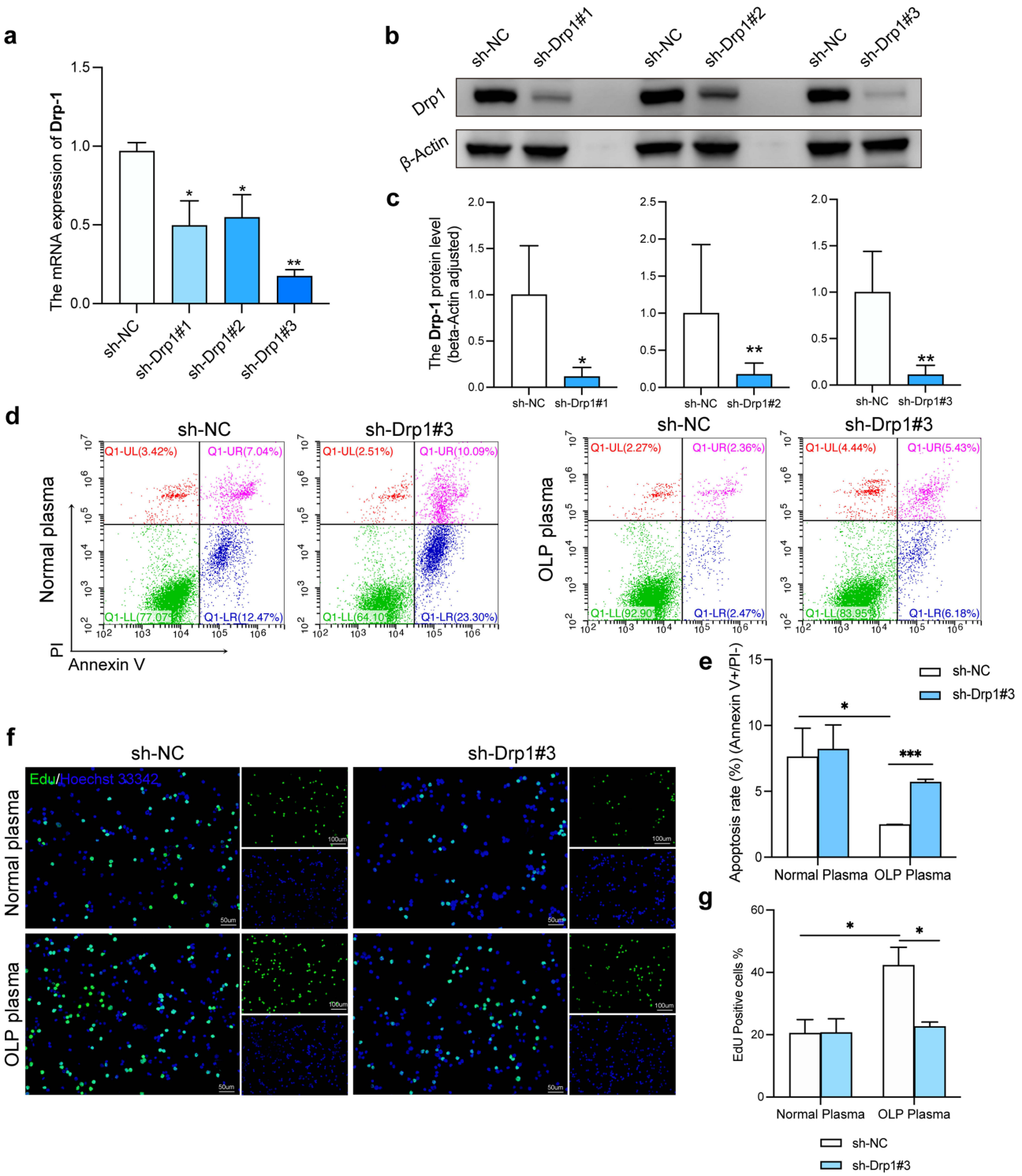

Figure 4 Effect of OLP plasma stimulation combined with Drp1 knockdown on T cell apoptosis and proliferation. Jurkat T cells were infected with either the negative control virus or Drp1 shRNA virus, then activated and cultured in OLP or normal plasma for 48 h. (**a**) Drp1 mRNA expression was detected by RT-qPCR (n = 3). (**b**) Representative images of Drp1 protein expression detected by Western blot. (**c**) Grey-scale analysis of Drp1/β-actin ratios (n = 3). (**d**) Apoptosis rates of sh-NC and sh-Drp1 Jurkat T cells cultured in OLP or normal plasma (n = 3), detected by flow cytometry. (**e**) Histogram showing the apoptosis rates (Annexin V+/PI-) of Jurkat T cells. (**f**) EdU cell proliferation staining of sh-NC and sh-Drp1 Jurkat T cells cultured in OLP or normal plasma (n = 4), detected by fluorescence microscopy. (**g**) Histogram showing the EdU Positive cells. sh-NC: Jurkat T cells infected with the negative control virus; sh-Drp1: Jurkat T cells infected with the Drp1 shRNA virus. **P* < 0.05, ***P* < 0.01, ****P* < 0.001.

Abbreviations: OLP, Oral Lichen Planus; β-Actin, Beta-Actin; Drp1, Dynamin-related protein 1; PI, Propidium Iodide.

stimulated with OLP plasma increased significantly compared to the sh-NC group with OLP plasma ($P < 0.0001$, Figure 4d and e).

Regarding cell proliferation, the EdU-positive cells in the sh-NC group stimulated with OLP plasma were higher than in the sh-NC group with normal plasma ($P = 0.0388$, Figure 4f and g), indicating active proliferation of T cells in OLP. Following Drp1 knockdown, cell proliferation decreased in the sh-Drp1 group stimulated with OLP plasma compared to the sh-NC group treated with OLP plasma ($P = 0.0294$, Figure 4f and g). These findings suggest that inhibiting DRP1-mediated mitochondrial fission could induce apoptosis and inhibit proliferative activity in OLP T cells.

OLP Plasma Stimulation Reduced Mitochondrial Respiration and Inhibited Apoptosis of T Cells by Decreasing NAD^+

JC-1 assays that detect mitochondrial membrane potential (MMP)[30] showed that MMP was lower in Jurkat T cells cultured with OLP plasma than normal controls. NMN treatment increased MMP in OLP plasma-cultured Jurkat T cells; however, FK866 decreased MMP in cells cultured with normal plasma (Figure 5a). Mitochondrial transcription factor A (mtTFA), a nuclear gene essential for mitochondrial respiration and DNA replication,[11] was downregulated in OLP plasma-cultured Jurkat T cells compared to normal controls ($P < 0.05$). Its expression level was restored by NMN treatment in OLP plasma and reduced by FK866 in normal plasma ($P < 0.05$, Figure 5b and c).

Apoptosis (Annexin V+/PI-) was significantly lower in Jurkat T cells cultured with OLP plasma than in normal controls (P = 0.0007). NMN treatment increased the apoptosis rate in OLP plasma-cultured Jurkat T cells (P = 0.0374,

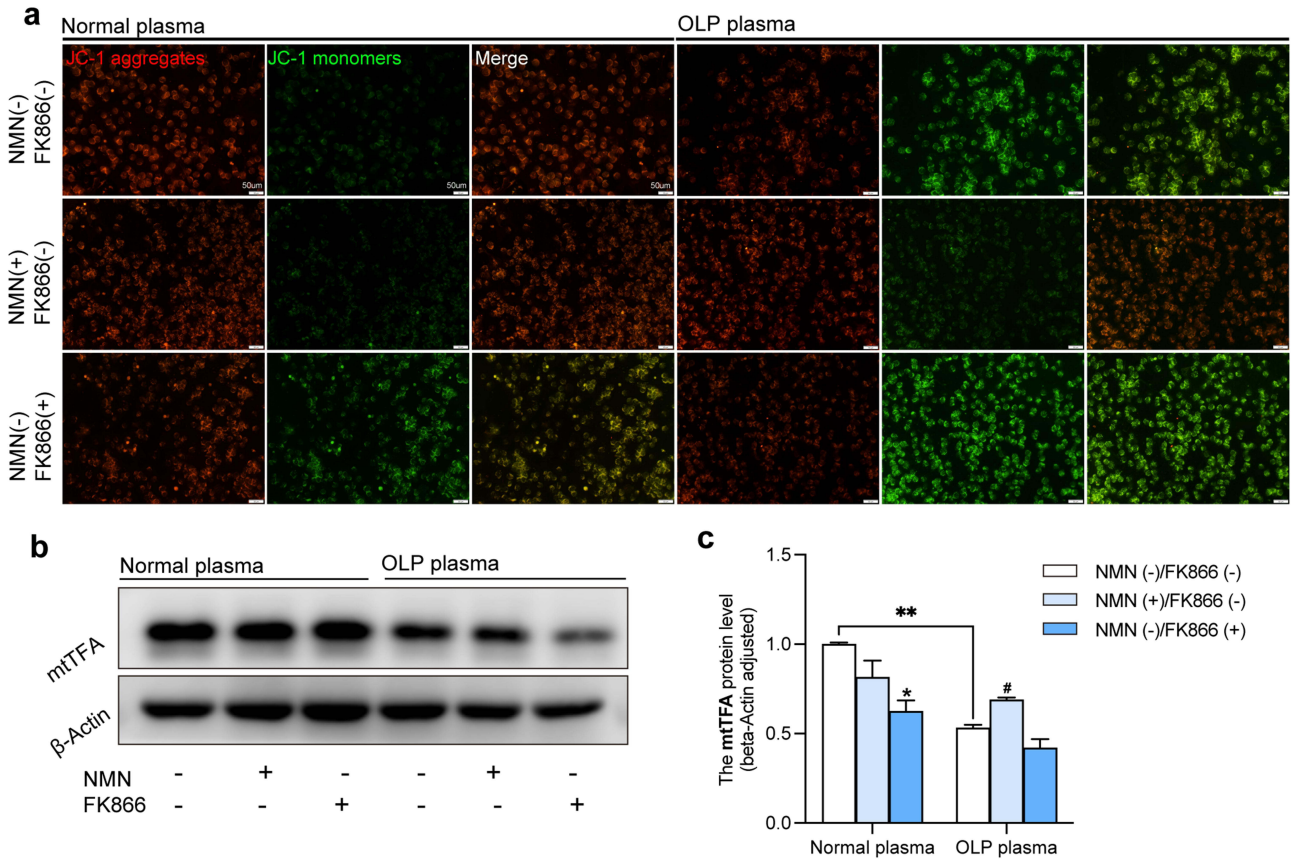

Figure 5 Effect of OLP plasma stimulation and NAD^+ levels on mitochondrial function. Activated Jurkat T cells were cultured in OLP or normal plasma and stimulated with NMN (0.5 mM) or FK866 (50 nM) for 48 h. (**a**) JC-1 staining of Jurkat T cells cultured in OLP or normal plasma (n = 3), observed by fluorescence microscopy. Scale bar: 50 μm. (**b**) Representative Western blot images of mtTFA expression. (**c**) Grey-scale analysis of mtTFA/β-actin ratios (n = 3). *$P < 0.05$, **$P < 0.01$ vs Normal plasma, #$P < 0.05$ vs OLP plasma with NMN (-)/FK866 (-).

Abbreviations: OLP, Oral Lichen Planus; NAD^+, Nicotinamide Adenine Dinucleotide; β-Actin, Beta-Actin; mtTFA, Mitochondrial Transcription Factor A; NMN, β-nicotinamide mononucleotide.

https://doi.org/10.2147/JIR.S502273

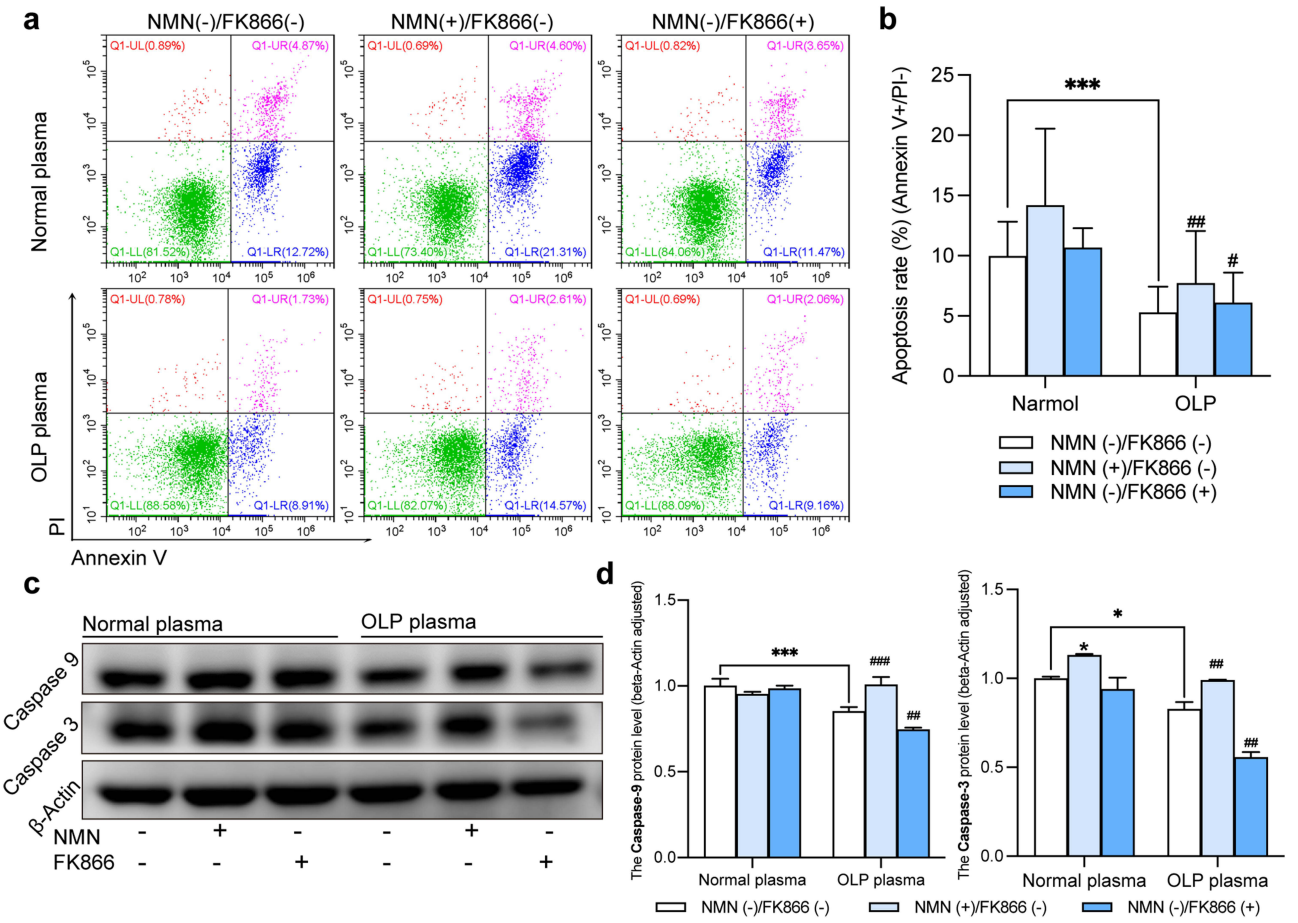

Figure 6 Effect of OLP plasma stimulation and NAD^+ levels on T cell apoptosis. Activated Jurkat T cells were cultured in OLP or normal plasma and stimulated with NMN (0.5 mM) or FK866 (50 nM) for 48 h. (**a**) Apoptosis rates of Jurkat T cells cultured in OLP or normal plasma (n = 6), detected by flow cytometry. (**b**) Histogram of apoptosis rates (Annexin V+/PI-) in Jurkat T cells. (**c**) Representative Western blot images of Caspase-9 and Caspase-3 expression. (**d**) Grey-scale analysis of Caspase-9/β-actin and Caspase-3/β-actin ratios (n = 3). $^*P < 0.05$, $^{***}P < 0.001$ vs Normal plasma, $^{\#}P < 0.05$, $^{\#\#}P < 0.01$, $^{\#\#\#}P < 0.001$ vs OLP plasma with NMN (-)/FK866 (-).
Abbreviations: OLP, Oral Lichen Planus; β-Actin, Beta-Actin; NMN, β-nicotinamide mononucleotide; PI, Propidium Iodide.

Figure 6a and b), correlating with increased protein levels of apoptosis-related proteins caspase-3 and caspase-9 ($P < 0.05$, Figure 6c and d). These findings suggest that OLP plasma impaired mitochondrial respiration and reduced apoptosis in T cells by decreasing NAD^+ levels and that NMN treatment could reverse this effect.

Discussion

In this study, OLP T cells exhibited mitochondrial fission. Mitochondrial fission exerts diverse regulatory effects on cells, with excessive Drp1-mediated mitochondrial fission leading to fragmentation and cell death.[31] However, in the present study, mitochondrial fission in OLP T cells was moderate and did not induce cell death. This moderate fission directly alters mitochondrial mass and function, driving a shift in cellular energy metabolism.[13] The present study showed that the mitochondria of OLP T cells decreased in mass and appeared small. Our previous study found elevated lactate dehydrogenase levels in the glycolytic pathway in OLP T cells.[8] Other studies have also suggested reduced oxidative phosphorylation sites due to mitochondrial fragmentation, resulting in a shift in energy metabolism of T cells toward glycolysis.[13] Thus, the metabolic profile transformation of T cells during OLP pathogenesis may depend on mitochondrial fission. Moreover, mitochondrial fission is associated with T cell activation. IL-2-activated T cells exhibit increased mitochondrial fission.[32] Consistently elevated IL-2 levels in OLP lesions[4] suggest a close relationship between T cell activation in OLP pathogenesis and mitochondrial fission. Mitochondrial fission also regulated the pro-inflammatory activity of immune cells through the NLRP3 inflammasome activation.[33] A previous study demonstrated significantly

higher levels of NLRP3 inflammasome in OLP patients.[34] Therefore, mitochondrial fission in T cells may be a pathogenic factor of OLP in multiple ways.

NAD^+ mediates mitochondrial biogenesis, dynamics, mitophagy, and other functions.[21] Many factors regulate mitochondrial fission, and NAD^+ is one of the most critical factors.[32] According to our findings, reduced NAD^+ levels in OLP T cells lead to mitochondrial fission, which can be reversed by NAD^+ supplementation. Other studies have confirmed that depolarization induced by low MMP can disrupt the electron transport chain, affecting mitochondrial function.[35] NAD^+ has been shown to restore MMP and improve mitochondrial function,[36] consistent with our findings. NAD^+ also plays an important role in autoimmune diseases. In SLE, decreased NAD^+ levels and low expression in mtTFA impair mitochondrial function in regulatory T cells.[37] NAD^+ can regulate mitochondria by catalyzing SIRT3.[21] The mitochondrial abnormalities caused by the decreased serum levels of SIRT3 may account for muscle dysfunction in patients with systemic sclerosis.[38] Taken together, the mitochondrial fission and the decrease in mitochondrial respiration induced by decreased NAD^+ may be involved in the pathogenesis of OLP.

Jurkat T cells cultured with OLP plasma exhibited similar mitochondrial fission as OLP T cells. Numerous recent studies have demonstrated elevated levels of inflammatory cytokines, including IL-1β and tumor necrosis factor (TNF)-α, in the serum of OLP patients.[39–42] Wang et al observed a significant increase in plasma levels of IL-1β in OLP patients.[43] TNF-α has been demonstrated to regulate intracellular NAD^+ level in macrophages by regulating the expression of NAD^+ homeostasis enzymes. Furthermore, IL-1β induces the expression of pro-inflammatory cytokines by upregulating SIRT1, a mammalian NAD^+-dependent deacetylase.[44] Conversely, NAD^+ supplementation reduces TNF-α and IL-1β levels in mice with Alzheimer's disease.[45] Therefore, a mutual feedback mechanism may exist between NAD^+ and inflammatory cytokines, including TNF-α and IL-1β. In this study, OLP plasma-stimulated Jurkat T cells showed low NAD^+ levels, increased mitochondrial fission, and mitochondrial dysfunction, which could be reversed by NMN. These findings demonstrated that inflammatory cytokines in OLP plasma may contribute to reducing NAD^+ levels in OLP T cells.

In this study, T cell apoptosis rates decreased in OLP, and NAD^+ supplementation induced apoptosis in OLP T cells. Concerning the fate of T cells, NAD^+ mainly regulated the activation, differentiation, and survival.[46] NAD^+ regulates cell apoptosis through dual mechanisms. NMN activates the NAD^+/SIRT1 pathway, attenuating apoptosis and inflammation in the hippocampal regions of septic mice.[26] Conversely, extracellular NAD^+ regulates T cell homeostasis by promoting NAD^+-induced cell death (NICD) in over-proliferating T cells.[47] At the same time, mitochondrial fission is a highly regulated process that can alter cell metabolism, proliferation, and apoptosis. Mitochondrial fission induces the biogenesis of new mitochondria and the removal of dysfunctional mitochondria through mitophagy, according to different states.[48] In OLP, T cells are activated, proliferate, migrate to lesion sites, and damage keratinocytes. NAD^+ may play a role in regulating mitochondrial fission and function in OLP T cells, inducing apoptosis in over-proliferating and activated T cells, finally restoring T cell homeostasis.

This study demonstrated for the first time that decreased NAD^+ levels contributed to mitochondrial fission in OLP T cells, providing new insights into OLP pathogenesis. NAD^+ supplementation reversed mitochondrial fission, restored mitochondrial function, and induced apoptosis, offering a potential therapeutic target for OLP. The study's main limitation was that OLP plasma was used to stimulate Jurkat T cells in vitro. Although Jurkat T cells exhibit many key characteristics of primary T cells, they do not completely replicate the complex disease state of OLP T cells. The inflammatory cytokines and others present in plasma also cannot fully emulate the immune-inflammatory environment of OLP.

Conclusion

In conclusion, this study demonstrated that reduced NAD^+ levels in OLP T cells suppressed apoptosis by promoting mitochondrial fission. NAD^+ supplementation reversed mitochondrial fission and enhanced T cell apoptosis, highlighting its potential as a therapeutic strategy to restore T cell homeostasis in OLP.

Data Sharing Statement

Data are available from corresponding authors upon reasonable request.

Ethics Approval

This research was complied with principles of the Declaration of Helsinki. It has been approved by the Ethics Committee of School and Hospital of Stomatology, Wuhan University (approval number 2022A30), and all subjects have signed informed consent forms.

Acknowledgments

The experimental facilities were partially supported by Core Facility of Medical Research Institute at Wuhan University, Research Center for Medicine and Structural Biology of Wuhan University. The abstract of this paper was presented at the 2024 FDI World Dental Congress as an oral presentation with interim findings. The abstract was published in 'Abstracts of the 2024 FDI World Dental Congress (Special Edition)' in International Dental Journal: https://www.sciencedirect.com/science/article/pii/S0020653924009882.

Author Contributions

All authors made a significant contribution to the work reported, whether that is in the conception, study design, execution, acquisition of data, analysis and interpretation, or in all these areas; took part in drafting, revising or critically reviewing the article; gave final approval of the version to be published; have agreed on the journal to which the article has been submitted; and agree to be accountable for all aspects of the work.

Declaration of Generative AI in Scientific Writing

There is no use of AI and AI-assisted technologies in the writing process.

Funding

This work was supported by the National Natural Science Foundation of China [grant numbers 82201067, 82270983, 82470982] and the special scholarship from Wuhan University for overseas postgraduate exchange programs.

Disclosure

The authors have no relevant financial or non-financial interests to disclose in this work.

References

1. Cheng LL. The proportion of oral lichen planus cases with malignant transformation may be higher, than reported to date. *J Evid Based Dent Pract*. 2022;22(2):101717. doi:10.1016/j.jebdp.2022.101717
2. Thongprasom K. Oral lichen planus: challenge and management. *Oral Dis*. 2018;24(1–2):172–173. doi:10.1111/odi.12712
3. Warnakulasuriya S, Kujan O, Aguirre-Urizar JM, et al. Oral potentially malignant disorders: a consensus report from an international seminar on nomenclature and classification, convened by the WHO Collaborating Centre for Oral Cancer. *Oral Dis*. 2021;27(8):1862–1880. doi:10.1111/odi.13704
4. El-Howati A, Thornhill MH, Colley HE, Murdoch C. Immune mechanisms in oral lichen planus. *Oral Dis*. 2023;29(4):1400–1415. doi:10.1111/odi.14142
5. Cheng YS, Gould A, Kurago Z, Fantasia J, Muller S. Diagnosis of oral lichen planus: a position paper of the American Academy of Oral and Maxillofacial Pathology. *Oral Surg Oral Med Oral Pathol Oral Radiol*. 2016;122(3):332–354. doi:10.1016/j.oooo.2016.05.004
6. Ghesquiere B, Wong BW, Kuchnio A, Carmeliet P. Metabolism of stromal and immune cells in health and disease. *Nature*. 2014;511(7508):167–176. doi:10.1038/nature13312
7. Zheng X, Qian Y, Fu B, et al. Mitochondrial fragmentation limits NK cell-based tumor immunosurveillance. *Nat Immunol*. 2019;20(12):1656–1667. doi:10.1038/s41590-019-0511-1
8. Wang F, Zhang J, Zhou G. 2-Deoxy-D-glucose impedes T cell-induced apoptosis of keratinocytes in oral lichen planus. *J Cell Mol Med*. 2021;25(21):10257–10267. doi:10.1111/jcmm.16964
9. Wang F, Zhang J, Zhou G. The mTOR-glycolytic pathway promotes T-cell immunobiology in oral lichen planus. *Immunobiology*. 2020;225(3):151933. doi:10.1016/j.imbio.2020.151933
10. Zhang Z, Li TE, Chen M, et al. MFN1-dependent alteration of mitochondrial dynamics drives hepatocellular carcinoma metastasis by glucose metabolic reprogramming. *Br J Cancer*. 2020;122(2):209–220. doi:10.1038/s41416-019-0658-4
11. Son JM, Sarsour EH, Kakkerla Balaraju A, et al. Mitofusin 1 and optic atrophy 1 shift metabolism to mitochondrial respiration during aging. *Aging Cell*. 2017;16(5):1136–1145. doi:10.1111/acel.12649
12. Galloway CA, Lee H, Yoon Y. Mitochondrial morphology-emerging role in bioenergetics. *Free Radic Biol Med*. 2012;53(12):2218–2228. doi:10.1016/j.freeradbiomed.2012.09.035

13. Angajala A, Lim S, Phillips JB, et al. Diverse roles of mitochondria in immune responses: novel insights into immuno-metabolism. *Front Immunol*. 2018;9:1605. doi:10.3389/fimmu.2018.01605
14. Nagdas S, Kashatus JA, Nascimento A, et al. Drp1 promotes kras-driven metabolic changes to drive pancreatic tumor growth. *Cell Rep*. 2019;28 (7):1845–1859e5. doi:10.1016/j.celrep.2019.07.031
15. De Benedittis G, Latini A, Colafrancesco S, et al. Alteration of mitochondrial DNA copy number and increased expression levels of mitochondrial dynamics-related genes in Sjogren's syndrome. *Biomedicines*. 2022;10(11):2699. doi:10.3390/biomedicines10112699
16. Caza TN, Fernandez DR, Talaber G, et al. HRES-1/Rab4-mediated depletion of Drp1 impairs mitochondrial homeostasis and represents a target for treatment in SLE. *Ann Rheum Dis*. 2014;73(10):1888–1897. doi:10.1136/annrheumdis-2013-203794
17. Alissafi T, Kalafati L, Lazari M, et al. Mitochondrial oxidative damage underlies regulatory T cell defects in autoimmunity. *Cell Metab*. 2020;32 (4):591–604e7. doi:10.1016/j.cmet.2020.07.001
18. De Biasi S, Simone AM, Bianchini E, et al. Mitochondrial functionality and metabolism in T cells from progressive multiple sclerosis patients. *Eur J Immunol*. 2019;49(12):2204–2221. doi:10.1002/eji.201948223
19. Navas LE, Carnero A. NAD(+) metabolism, stemness, the immune response, and cancer. *Signal Transduct Target Ther*. 2021;6(1):2. doi:10.1038/s41392-020-00354-w
20. Ralto KM, Rhee EP, Parikh SM. NAD(+) homeostasis in renal health and disease. *Nat Rev Nephrol*. 2020;16(2):99–111. doi:10.1038/s41581-019-0216-6
21. Klimova N, Fearnow A, Long A, Kristian T. NAD+ precursor modulates post-ischemic mitochondrial fragmentation and reactiv e oxygen species generation via SIRT3 dependent mechanisms. *Exp Neurol*. 2020;325:113144. doi:10.1016/j.expneurol.2019.113144
22. Khan NA, Auranen M, Paetau I, et al. Effective treatment of mitochondrial myopathy by nicotinamide riboside, a vitamin B3. *EMBO Mol Med*. 2014;6(6):721–731. doi:10.1002/emmm.201403943
23. Doke T, Mukherjee S, Mukhi D, et al. NAD(+) precursor supplementation prevents mtRNA/RIG-I-dependent inflammation during kidney injury. *Nat Metab*. 2023;5(3):414–430. doi:10.1038/s42255-023-00761-7
24. Zhou B, Wang DD, Qiu Y, et al. Boosting NAD level suppresses inflammatory activation of PBMCs in heart failure. *J Clin Invest*. 2020;130 (11):6054–6063. doi:10.1172/JCI138538
25. Ye B, Pei Y, Wang L, et al. NAD(+) supplementation prevents STING-induced senescence in CD8(+) T cells by improving mitochondrial homeostasis. *J Cell Biochem*. 2024;125(3):e30522. doi:10.1002/jcb.30522
26. Li H-R, Liu Q, Zhu C-L, et al. β-Nicotinamide mononucleotide activates NAD+/SIRT1 pathway and attenuates inflammatory and oxidative responses in the hippocampus regions of septic mice. *Redox Biol*. 2023;63:102745. doi:10.1016/j.redox.2023.102745
27. Pant K, Richard S, Peixoto E, et al. The NAMPT Inhibitor FK866 in combination with cisplatin reduces cholangiocarcinoma cells growth. *Cells*. 2023;12(5):775. doi:10.3390/cells12050775
28. Qin Z, Song J, Huang J, et al. Mitigation of triptolide-induced testicular Sertoli cell damage by melatonin via regulating the crosstalk between SIRT1 and NRF2. *Phytomedicine*. 2023;118:154945. doi:10.1016/j.phymed.2023.154945
29. Abraham RT, Weiss A. Jurkat T cells and development of the T-cell receptor signalling paradigm. *Nat Rev Immunol*. 2004;4(4):301–308. doi:10.1038/nri1330
30. Chen Z, Wang C, Yu N, et al. INF2 regulates oxidative stress-induced apoptosis in epidermal HaCaT cells by modulating the HIF1 signaling pathway. *Biomed Pharmacother*. 2019;111:151–161. doi:10.1016/j.biopha.2018.12.046
31. Liu Z, Li H, Su J, et al. Numb depletion promotes Drp1-mediated mitochondrial fission and exacerbates mitochondrial fragmentation and dysfunction in acute kidney injury. *Antioxid. Redox Signaling*. 2019;30(15):1797–1816. doi:10.1089/ars.2017.7432
32. Buck MD, O'Sullivan D, Klein Geltink RI, et al. Mitochondrial dynamics controls T cell fate through metabolic programming. *Cell*. 2016;166 (1):63–76. doi:10.1016/j.cell.2016.05.035
33. Park S, Won JH, Hwang I, Hong S, Lee HK, Yu JW. Defective mitochondrial fission augments NLRP3 inflammasome activation. *Sci Rep*. 2015;5 (1):15489. doi:10.1038/srep15489
34. Thi Do T, Phoomak C, Champattanachai V, Silsirivanit A, Chaiyarit P. New evidence of connections between increased O-GlcNAcylation and inflammasome in the oral mucosa of patients with oral lichen planus. *Clin Exp Immunol*. 2018;192(1):129–137. doi:10.1111/cei.13091
35. Castro-Portuguez R, Sutphin GL. Kynurenine pathway, NAD(+) synthesis, and mitochondrial function: targeting tryptophan metabolism to promote longevity and healthspan. *Exp Gerontol*. 2020;132:110841. doi:10.1016/j.exger.2020.110841
36. Luengo A, Li Z, Gui DY, et al. Increased demand for NAD(+) relative to ATP drives aerobic glycolysis. *Mol Cell*. 2021;81(4):691–707e6. doi:10.1016/j.molcel.2020.12.012
37. Li W, Gong M, Park YP, et al. Lupus susceptibility gene Esrrg modulates regulatory T cells through mitochondrial metabolism. *JCI Insight*. 2021;6 (14). doi:10.1172/jci.insight.143540
38. Khodaei F, Rashedinia M, Heidari R, Rezaei M, Khoshnoud MJ. Ellagic acid improves muscle dysfunction in cuprizone-induced demyelinated mice via mitochondrial Sirt3 regulation. *Life Sci*. 2019;237:116954. doi:10.1016/j.lfs.2019.116954
39. Hu JY, Zhang J, Cui JL, et al. Increasing CCL5/CCR5 on CD4+ T cells in peripheral blood of oral lichen planus. *Cytokine*. 2013;62(1):141–145. doi:10.1016/j.cyto.2013.01.020
40. Wang Y, Zhang H, Du G, et al. Total glucosides of paeony (TGP) inhibits the production of inflammatory cytokines in oral lichen planus by suppressing the NF-kappaB signaling pathway. *Int Immunopharmacol*. 2016;36:67–72. doi:10.1016/j.intimp.2016.04.010
41. Zhang Y, Lin M, Zhang S, et al. NF-kappaB-dependent cytokines in saliva and serum from patients with oral lichen planus: a study in an ethnic Chinese population. *Cytokine*. 2008;41(2):144–149. doi:10.1016/j.cyto.2007.11.004
42. Rhodus NL, Cheng B, Myers S, Bowles W, Ho V, Ondrey F. A comparison of the pro-inflammatory, NF-kappaB-dependent cytokines: TNF-alpha, IL-1-alpha, IL-6, and IL-8 in different oral fluids from oral lichen planus patients. *Clin Immunol*. 2005;114(3):278–283. doi:10.1016/j.clim.2004.12.003
43. Wang ZM, Zhang J, Wang F, Zhou G. The tipped balance of ILC1/ILC2 in Peripheral blood of oral lichen planus is related to inflammatory cytokines. *Front Cell Dev Biol*. 2021;9:725169. doi:10.3389/fcell.2021.725169
44. Jung J, Lee YH, Fang X, et al. IL-1beta induces expression of proinflammatory cytokines and migration of human colon cancer cells through upregulation of SIRT1. *Arch Biochem Biophys*. 2021;703:108847. doi:10.1016/j.abb.2021.108847

45. Hou YJ, Wei Y, Lautrup S, et al. NAD plus supplementation reduces neuroinflammation and cell senescence in a transgenic mouse model of Alzheimer's disease via cGAS-STING. *Proc Natl Acad Sci U S A*. 2021;118(37). doi:ARTNe2011226118.doi:10.1073/pnas.2011226118.
46. Rodriguez Cetina Biefer H, Heinbokel T, Uehara H, et al. Mast cells regulate CD4(+) T-cell differentiation in the absence of antigen presentation. *J Allergy Clin Immunol*. 2018;142(6):1894–1908e7. doi:10.1016/j.jaci.2018.01.038
47. Nation CS, Da'Dara AA, Skelly PJ. The essential schistosome tegumental ectoenzyme SmNPP5 can block NAD-induced T cell apoptosis. *Virulence*. 2020;11(1):568–579. doi:10.1080/21505594.2020.1770481
48. Kleele T, Rey T, Winter J, et al. Distinct fission signatures predict mitochondrial degradation or biogenesis. *Nature*. 2021;593:7859):435–439. doi:10.1038/s41586-021-03510-6